

## Unified Kraft Break at $\sim 6500$ K: A Newly Identified Single-Star Obliquity Transition Matches the Classical Rotation Break

XIAN-YU WANG (汪宪钰) <sup>1,\*</sup> SONGHU WANG (王松虎) AND J. M. JOEL ONG (王加冕) <sup>2,3</sup>

<sup>1</sup>*Department of Astronomy, Indiana University, 727 East 3rd Street, Bloomington, IN 47405-7105, USA*

<sup>2</sup>*Sydney Institute for Astronomy (SIfA), School of Physics, University of Sydney, NSW 2006, Australia*

<sup>3</sup>*Institute for Astronomy, University of Hawai'i, 2680 Woodlawn Drive, Honolulu, HI 96822, USA*

### ABSTRACT

The stellar obliquity transition, defined by a  $T_{\text{eff}}$  cut separating aligned from misaligned hot Jupiter systems, has long been assumed to coincide with the rotational Kraft break. Yet the commonly quoted obliquity transition (6100 or 6250 K) sits a few hundred kelvin cooler than the rotational break ( $\sim 6500$  K), posing a fundamental inconsistency. We show this offset arises primarily from *binaries/multiple-star systems*, which drive the cooler stellar obliquity transition ( $6105^{+123}_{-133}$  K), although the underlying cause remains ambiguous. After removing binaries and higher-order multiples, the single-star stellar obliquity transition shifts upward to  $6447^{+85}_{-119}$  K, in excellent agreement with the single-star rotation break ( $6510^{+97}_{-127}$  K). This revision has two immediate consequences for understanding the origin and evolution of spin-orbit misalignment. First, the upward shift reclassifies some hosts previously labeled ‘hot’ into the cooler regime; consequently, there are *very* few RM measurements of non-hot-Jupiter planets around genuinely hot stars ( $T_{\text{eff}} \gtrsim 6500$  K), and previously reported alignment trends for these classes of systems (e.g., warm Jupiters and compact multi-planet systems) lose the power to discriminate the central question: are large misalignments unique to hot-Jupiter-like planets that can be delivered by high- $e$  migration, or are hot stars intrinsically more misaligned across architectures? Second, a single-star stellar obliquity transition near 6500 K, coincident with the rotational break, favors tidal dissipation in outer convective envelopes; as these envelopes thin with increasing  $T_{\text{eff}}$ , inertial-wave damping and magnetic braking weaken in tandem.

**Keywords:** exoplanet systems (484), exoplanet dynamics (490), exoplanets (498), planetary alignment (1243), planetary theory (1258), stellar structures (1631), star-planet interactions (2177)

### 1. INTRODUCTION

The mass of a star largely determines how it *generates* energy, and how this energy is *transported*. Relatively low core temperatures in low-mass cool dwarfs ( $0.5 - 1.3 M_{\odot}$ ) favor hydrogen burning through the proton-proton chain, with energy carried outward through a deep convective envelope. In hotter, more massive dwarfs, the CNO cycle dominates hydrogen burning in a convective core, while the overlying envelope is predominantly radiative. These structural differences have been supported by multiple observational tracers. For

example, cool dwarfs show envelope-driven mixing that depletes surface lithium (Boesgaard & Tripicco 1986; Hobbs & Pilachowski 1986; Deliyannis & Pinsonneault 1997; Sestito & Randich 2005). Where asteroseismology is observationally available, this convection stochastically excites solar-like oscillations (Kjeldsen & Bedding 1995; Chaplin & Miglio 2013; Silva Aguirre et al. 2013). Hotter F stars, with shallower convective envelopes, exhibit far shorter convective turnover and damping timescales in their pulsations. Stars which are hotter still possess negligible convective envelopes, and display only classical pulsations (e.g.  $\delta$  Scuti/roAp) driven by the  $\kappa$  mechanism (Cox 1980).

A much more easily accessible observational manifestation of this structural shift is the sharp drop in rotation rates at mid-F spectral types: the well-known

Corresponding author: Songhu Wang  
 sw121@iu.edu

\* Sullivan Prize Postdoctoral Fellow

*Kraft break*<sup>1</sup> (Kraft 1967). A sufficiently thick convective envelope in cool stars sustains a global magnetic dynamo, whose efficiency is described by the dimensionless Rossby number, operationally defined as the ratio between the rotational period and the convective turnover timescale (Noyes et al. 1984; Brun & Browning 2017). Low Rossby numbers in cool stars are generally associated with higher magnetic activity, manifesting as enhanced spots, frequent flares, and strong chromospheric/coronal emission (e.g. Saar & Brandenburg 1999; Pizzolato et al. 2003; Mamajek & Hillenbrand 2008; Reiners et al. 2009; Vidotto et al. 2014; Stelzer et al. 2016; Newton et al. 2017; Feinstein et al. 2020; See et al. 2023; Mathur et al. 2025). Magnetized stellar winds extract angular momentum and slow the rotation of stars as they age (e.g. Weber & Davis 1967; Skumanich 1972; Kawaler 1989; Barnes 2003; van Saders & Pinsonneault 2013). By contrast, with thinner convective envelopes, magnetic braking is much less efficient in hot stars, which remain rapidly rotating on the main sequence.

Independently, exoplanet observations have revealed a transition in the stellar spin-orbit angle, the angle between the stellar rotation axis and the planetary orbital axis (hereafter obliquity), among host stars: hot Jupiters orbiting hotter stars more likely exhibit large misalignments, whereas those around cooler stars are usually well aligned (e.g., Schlaufman 2010; Winn et al. 2010a; Albrecht et al. 2012, 2021; Knudstrup et al. 2024). This is often attributed to efficient tidal obliquity damping (Albrecht et al. 2012), via dissipation of tidally excited inertial waves within convective envelopes (Ogilvie & Lin 2007; Lai 2012; Li & Winn 2016; Saunders et al. 2024), and, where relevant, by resonances between the dynamical tides and stellar oscillations (Zanazzi et al. 2024; Zanazzi & Chiang 2025), whereas such damping is inefficient in hot, radiative-envelope stars.

Because both phenomena reflect a structural break separating cool and hot stars, it has long been assumed that the *rotation* and *obliquity* transitions coincide. Whether they do has remained unclear. Historically, both the rotation (e.g., Kraft 1967; Noyes et al. 1984; van Saders & Pinsonneault 2013; Avallone et al. 2022) and obliquity (e.g., Winn et al. 2010a; Albrecht et al. 2012; Winn & Fabrycky 2015; Triaud 2018; Albrecht et al. 2022; Knudstrup et al. 2024) literatures have been content to adopt notional thresholds without

fitting them statistically, leading to somewhat disparate breaks: a mid-F (i.e.  $M_\star = 1.2\text{--}1.3 M_\odot$ ) divider, or the equivalent in color or temperature (such as  $B-V = 0.3$ ,  $G_{\text{BP}}-G_{\text{RP}} = 0.55\text{--}0.60$ , or  $T_{\text{eff}} \sim 6500$  K: Iben 1967; do Nascimento et al. 2000; van Saders et al. 2019) for rotation, and  $T_{\text{eff}} = 6000\text{--}6300$  K (often 6100 or 6250 K, as reviewed by Albrecht et al. 2022) for obliquity, without a formal turning-point inference or quoted uncertainties.

Recent work has sharpened one side of this picture. Using a carefully curated sample of nearby single F-dwarfs, Beyer & White (2024) found a sharp rotation transition centered at  $T_{\text{eff}} = 6550$  K (width of 200 K), arguing that the commonly cited 6100 K obliquity transition is 450 K cooler than this value. Although the obliquity sample (dominated by hot-Jupiter hosts) and the rotation sample (composed of F stars within 33 pc) do differ in [Fe/H] (medians  $0.04^{+0.20}_{-0.16}$  vs.  $-0.15^{+0.19}_{-0.18}$ ) — which can affect the Kraft-break location by altering envelope opacity (and thus convective-zone depth and magnetic-braking efficiency) — a  $\sim 0.2$  dex metallicity offset is expected to shift the break only by less than 100 K (Spalding & Winn 2022): far smaller than the observed 450 K gap.

We notice that the rotation result pertains to a rigorously vetted sample of *single* stars. The often-cited obliquity divider near 6100 K, however, is typically drawn from literature samples that include binaries and multiple-star systems. As a result, a direct apples-to-apples comparison between the rotation and obliquity breaks in single-star systems does not yet exist.

In this work, we supply one: we present a consistent statistical determination of the transition points in both stellar  $v \sin i_\star$  (rotation) and  $\lambda$  (obliquity), enabling a rigorous comparison of like with like. We apply a uniform “turning-point” fitting methodology to an updated, single-star rotation sample based on Beyer & White (2024), and confirm a sharp rotation transition at  $T_{\text{eff}} = 6510^{+97}_{-127}$  K. Applying the same procedure to a hot-Jupiter Rossiter-McLaughlin (RM, Rossiter 1924; McLaughlin 1924) sample, we recover an obliquity transition consistent with commonly quoted values,  $T_{\text{eff}} = 6105^{+123}_{-133}$  K. Thus, our baseline analysis reproduces a similar but slightly smaller 405 K offset to that noted by Beyer & White (2024). Crucially, when we remove binaries from the obliquity sample so that both probes refer to *single* stars, the inferred obliquity break shifts upward to  $T_{\text{eff}} = 6447^{+85}_{-119}$  K, which is statistically indistinguishable from the rotation break ( $6510^{+97}_{-127}$  K), differing by only  $0.41\sigma$ . That is to say, a *single* mid-F boundary at  $\sim 6500$  K consistently describes both the rotation (Kraft) break and the spin-orbit alignment transition, once binarity is controlled for.

<sup>1</sup> Explicit evidence for a sharp drop in rotation near F5 long predates Kraft’s work (e.g., Struve & Elvey 1931; Westgate 1934).

## 2. SAMPLE CONSTRUCTION

### 2.1. Stellar Rotation, $v \sin i_*$

To statistically identify the turning point of the Kraft rotation break, we assembled a sample of 405 systems with  $T_{\text{eff}}$  and  $v \sin i_*$  measurements (panels c and d of Figure 1), following the general selection and vetting criteria described in Section 2 of Beyer & White (2024), but with minor modifications aimed at expanding the sample and minimizing the influence of binary/multiple-star systems.

We compiled all bright F-type stars within 33.33 pc of the Sun that have reliable parallax measurements, using the ADQL query described in Section 2 of Beyer & White (2024). The primary source of  $T_{\text{eff}}$  is `teff_gsphot`; if unavailable, we adopt `teff_gsspec` or `teff_esphs`<sup>2</sup>. If none of these are available,  $T_{\text{eff}}$  values from the Geneva–Copenhagen Survey (Nordström et al. 2004) and the stellar property catalog of rapidly rotating Sun-like stars by Schröder et al. (2009) were supplemented. As for  $v \sin i_*$ , the Gaia DR3 line-broadening measurements (`vbroad`) were adopted as a proxy (Frémat et al. 2023). When `vbroad` was unavailable, we instead used  $v \sin i_*$  values from Nordström et al. (2004) and Schröder et al. (2009). Following Beyer & White (2024), we removed young stars (with ages less than 200 Myr) and evolved stars (with  $\log g_* < 3.75$ ), as these may exhibit anomalous rotation rates. We identified systems with stellar companions via multiple steps. Firstly, binaries and binary candidates were identified by cross-matching our targets with the Geneva–Copenhagen Survey (Nordström et al. 2004), where entries marked with an asterisk in the  $f_d$  (confirmed or suspected binaries) or  $f_b$  (spectroscopic binaries) flags were considered binary or potential binary systems. Next, we identified stellar companions following the methods described in El-Badry et al. (2021), but without the  $G < 18$  limitation in order to include faint stellar companions. Finally, stars with Renormalized Unit Weight Error (RUWE, Lindegren et al. 2018, 2021)  $> 1.4$  were classified as potential binary or multiple-star systems. The final sample comprises 405 stars with  $T_{\text{eff}}$  and  $v \sin i_*$  measurements, including 182 mature, single main-sequence stars, 206 binary or multiple-star systems (see panels c and d of Figure 1), and 17 young or evolved stars, which are excluded from our analysis.

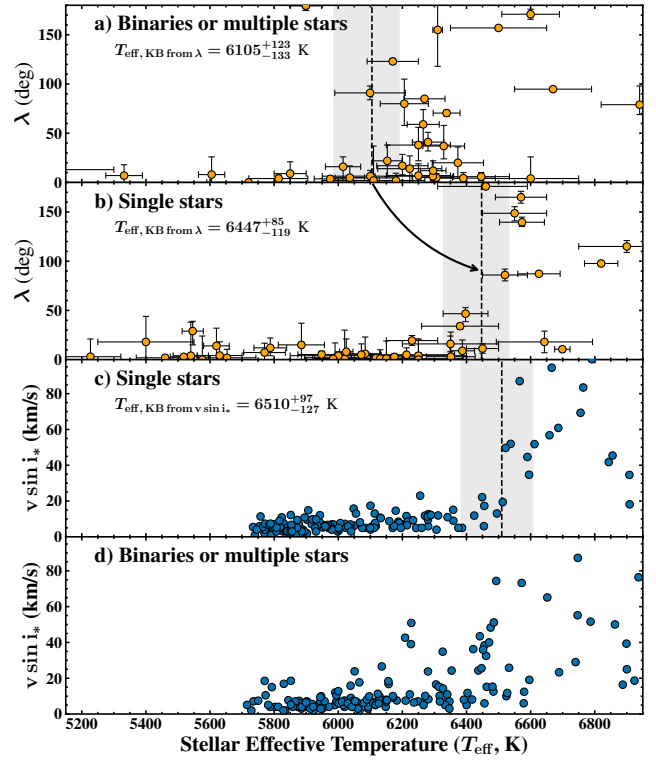


**Figure 1.** The  $\lambda$  and  $v \sin i_*$  distributions, along with derived  $T_{\text{eff}}$  boundaries. *Panel a:*  $\lambda$  distribution for hot-Jupiter systems with confirmed or candidate stellar companions. The  $T_{\text{eff}}$  boundary of  $6105^{+123}_{-133}$  K is marked with a black dashed line, with shaded  $1\sigma$  interval. *Panel b:* Same as the top panel, but for single-star hot-Jupiter systems with  $T_{\text{eff}}$  boundary =  $6447^{+85}_{-119}$  K. *Panel c:*  $v \sin i_*$  distribution for single stars, compiled following the updated prescription described in Beyer & White (2024). The resulting  $T_{\text{eff}}$  boundary is  $6510^{+97}_{-127}$  K, consistent with that derived from the single-star  $\lambda$  distribution. *Panel d:* same as panel c, but for binary and multiple-star systems.

### 2.2. Stellar Obliquity, $\lambda$

To determine the boundary of the obliquity transition, we focus on systems that would be affected by tidal realignment, if operative. Concretely, we select hot Jupiters with mass ratios  $3 \times 10^{-4} \leq m_p/M_* \leq 2 \times 10^{-3}$  (Rusznak et al. 2025) on close-in orbits with  $a/R_* < 10$ , and with measured stellar obliquities. Stellar masses, planetary masses, and  $a/R_*$  are taken from the Planetary Systems Composite Parameters table (PSCompPars<sup>3</sup>, NASA Exoplanet Archive 2019) at NASA Exoplanet Archive (Christiansen et al. 2025); when a value is missing there, we adopt the entry from

<sup>2</sup> [https://gaia.aip.de/metadata/gaiadr3/astrophysical\\_parameters/](https://gaia.aip.de/metadata/gaiadr3/astrophysical_parameters/)

<sup>3</sup> <https://exoplanetarchive.ipac.caltech.edu/cgi-bin/TblView/nph-tblView?app=ExoTbls&config=PSCompPars>

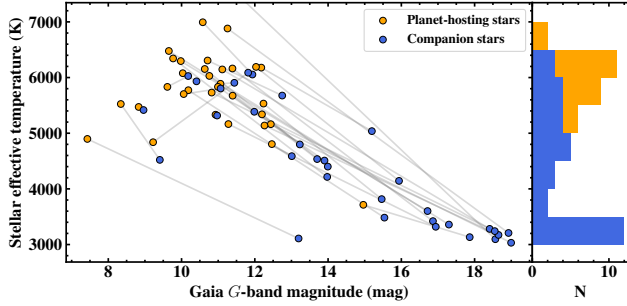


**Figure 2.** Stellar effective temperature ( $T_{\text{eff}}$ ) and Gaia DR3  $G$  magnitude for the stellar obliquity sample with stellar companions. Planet-host stars and their corresponding stellar companions are shown as orange and blue dots, respectively. The  $T_{\text{eff}}$  distributions of the two populations are shown in the right panel. Interestingly, in our stellar-obliquity sample (consisting of hot Jupiters), the planet host is *always* the more massive component of a binary.

the Encyclopaedia of exoplanetary systems<sup>4</sup> as a fallback.

Among stellar-obliquity measurement techniques, the Rossiter-McLaughlin method is the most widely used and provides the majority of  $\lambda$  measurements (Winn & Fabrycky 2015; Triaud 2018; Albrecht et al. 2022). Because different techniques introduce different selection effects (e.g., spot-crossing is more sensitive to aligned systems, while gravity-darkening is usually significant only for highly misaligned systems, Siegel et al. 2023; Albrecht et al. 2022), we retain only RM-based measurements, giving priority in the following order: classical RM, Doppler shadow (Albrecht et al. 2007; Collier Cameron et al. 2010; Zhou et al. 2016; Johnson et al. 2017), reloaded RM (Cegla et al. 2016), and RM Revolution (Bourrier et al. 2021). For all retained systems, we adopt the sky-projected obliquity  $\lambda$  and  $T_{\text{eff}}$  from TEPCat<sup>5</sup> (Southworth 2011).

Following Albrecht et al. (2022), we exclude low-precision measurements with  $\sigma_{\lambda} > 50^\circ$  and controversial cases flagged in the literature: CoRoT-1 (Bouchy et al. 2009) reported an aligned configuration, while Pont et al. 2010 found a significant misalignment of  $\lambda = 77 \pm 11^\circ$ , CoRoT-19 (Guenther et al. 2012, the RM effect was detected at only a  $2.3\sigma$  confidence level), HATS-14 (Zhou et al. 2015, the  $\lambda$  constraint is sensitive to the  $v \sin i_*$  prior and RM offset modeling due to the lack of post-egress data), HAT-P-27 (Brown et al. 2012,

large  $\lambda$  uncertainty:  $\lambda = 24.2^{+76.0^\circ}_{-44.5^\circ}$ ), HD 3167 (a large mutual inclination of  $\sim 100^\circ$  was inferred from literature  $\lambda$  measurements, Dalal et al. 2019 and Bourrier et al. 2021, although Teng et al. 2025 showed that such a configuration is unlikely to be maintained), WASP-1 (Simpson et al. 2011; Albrecht et al. 2011, a weak signal of a prograde orbit was detected with  $\sim 2\sigma$  confidence), WASP-2 (Triaud et al. 2010; Albrecht et al. 2011, no RM signal was detected), WASP-23 (Triaud et al. 2011, the  $\lambda$  constraint is sensitive to the  $v \sin i$  prior due to the low transit impact parameter), WASP-49 (Wyttenbach et al. 2017, large  $\lambda$  uncertainty:  $\lambda = 54^{+79^\circ}_{-58^\circ}$ ), WASP-134 (Anderson et al. 2018, the  $\lambda$  constraint is sensitive to assumptions on priors and RM offset due to the lack of post-egress data), and HAT-P-17 (an aligned configuration of  $\lambda = 19^{+14^\circ}_{-16^\circ}$  was initially reported by Fulton et al. 2013, but a misalignment of  $\lambda = -27.5 \pm 6.7^\circ$  was later found by Mancini et al. 2022)

Stellar multiplicity has long been theorized as a potential driver of spin-orbit misalignments (Holman et al. 1997; Wu & Murray 2003; Fabrycky & Tremaine 2007; Naoz et al. 2012; Batygin 2012). Recent obliquity studies confirm that warm Jupiters tend to be aligned in single-star systems (Rice et al. 2022; Wang et al. 2024; Espinoza-Retamal et al. 2023) yet are frequently (and sometimes famously, e.g., HD 80606; Winn et al. 2009; TIC 241249530; Gupta et al. 2024) misaligned in binaries; massive planets show a similar single-versus-binary contrast (Rusznak et al. 2025). Motivated by this, we identify and flag binaries or higher-order multiples in our obliquity sample using Schwarz et al. (2016) and Fontanive & Bardalez Gagliuffi (2021). Similar to subsection 2.1, we examined the binarity of each system following the method of El-Badry et al. (2021), but extended it to include faint nearby stars ( $G > 18$ ). We also classified systems with  $\text{RUWE} > 1.4$  as binary candidates. Moreover, we only include systems with stellar ages  $> 200$  Myr and  $\log g_* > 3.75$  to exclude young and evolved stars, which is consistent with the construction of the  $v \sin i_*$  sample.

After excluding poor or controversial obliquity measurements, as well as young and evolved stars, the hot-Jupiter obliquity samples used for our turning-point analysis consist of 91 systems in total, of which 50 are single-star systems (See panels a and b of Figure 1).

### 3. $T_{\text{eff}}$ BOUNDARY DETERMINATION

To identify the  $T_{\text{eff}}$  boundary that best separates cool (low  $v \sin i_*$ , aligned) and hot (high  $v \sin i_*$ , misaligned) systems, we evaluated candidate cuts at the midpoints between adjacent unique  $T_{\text{eff}}$  values in each statistical test.

<sup>4</sup> <https://exoplanet.eu/catalog/>

<sup>5</sup> <https://www.astro.keele.ac.uk/jkt/tepcat/obliquity.html>, accessed on 2025 October 04.

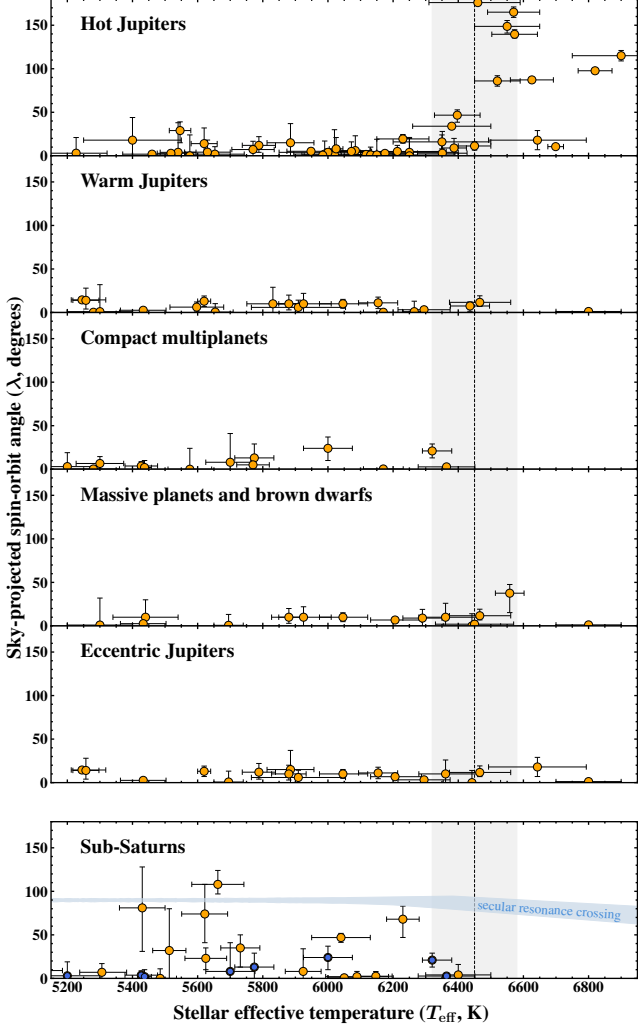


**Figure 3.** The  $\lambda$  distributions for hot-Jupiter ( $3 \times 10^{-4} \leq m_p/M_\star \leq 2 \times 10^{-3}$ ,  $a/R_\star < 10$ ), sub-Saturn ( $3 \times 10^{-5} \leq m_p/M_\star \leq 3 \times 10^{-3}$ ), warm-Jupiter ( $3 \times 10^{-4} \leq m_p/M_\star \leq 2 \times 10^{-3}$ ,  $a/R_\star > 11$ ), compact multiplanet (period ratio of adjacent planets,  $P_{i+1}/P_i < 6$ ), massive-planet systems ( $2 \times 10^{-3} \leq m_p/M_\star$ ), and eccentric Jupiters ( $3 \times 10^{-4} \leq m_p/M_\star \leq 2 \times 10^{-3}$ ,  $e > 0.1$ ), along with the Kraft break and its associated uncertainty derived in this work. In terms of  $T_{\text{eff}}$  coverage, only the hot-Jupiter systems have sufficient measurements ( $> 10$ ) in the hot-star regime. Sub-Saturns with nearby companions are marked in blue. The predicted relation between  $T_{\text{eff}}$  and  $\lambda$  from secular resonance crossing (Petrovich et al. 2020; Dugan et al. 2025) is shown as the light-blue shaded region.

For each candidate cut, we required at least five systems in both the cool and hot populations to ensure adequate sample sizes. We then compared the  $\lambda$  or  $v \sin i_\star$  distributions of the two populations using the two-sample Kolmogorov-Smirnov (KS; Hodges 1958) test as implemented in `scipy` (Virtanen et al. 2020). We quantified the statistical significance as  $-\log_{10}(p)$ , where  $p$

is the KS test  $p$ -value, since the logarithmic scale facilitates comparison across small  $p$ -values. We defined the optimal boundary as the  $T_{\text{eff}}$  cut that maximized this quantity.

To estimate the uncertainty in the optimal boundary, we performed a bootstrap analysis. We generated 100,000 bootstrap realizations by resampling the targets with replacement. In each realization, we perturbed every star’s  $T_{\text{eff}}$  by drawing from a Gaussian distribution centered on its reported value with standard deviation equal to its measurement uncertainty (i.e.,  $\sigma_{T_{\text{eff}}}$ ). Note that a conservative 2.4% floor uncertainty in  $T_{\text{eff}}$  was adopted (Tayar et al. 2022). For each bootstrap sample, we repeated the boundary search over the same  $T_{\text{eff}}$  grid and identified the turning point that maximized the two-sample KS statistic. The resulting distribution of 100,000 turning points was then used to derive the cut and the corresponding lower and upper uncertainties.

We applied this procedure to the stellar-obliquity distribution of hot-Jupiter systems whose hosts had stellar companions (Figure 1, panel a) and obtained a boundary at  $6105^{+123}_{-133}$  K, consistent with the commonly quoted  $6100 - 6250$  K range, confirming that the previously reported obliquity transition  $T_{\text{eff}}$  is driven by hot-Jupiter systems in binaries. For hot Jupiters around single stars (Figure 1, panel b), the turning point of their obliquity distribution is  $6447^{+85}_{-119}$  K, in excellent agreement with the  $v \sin i_\star$  break for single stars that we measure at  $6510^{+97}_{-127}$  K (Figure 1, panel c).

#### 4. WHY THE BREAK LOOKS COOLER IN BINARY SAMPLES

Our statistical analysis shows that, when we restrict the sample to *single stars*, the Kraft rotation break and the obliquity transition coincide near  $T_{\text{eff}} \sim 6500$  K (see Figure 1, panels b and c). In contrast, for *binaries and higher-order multiples*, the misaligned fraction rises sharply above  $T_{\text{eff}} \sim 6100$  K, matching the often-quoted threshold that our results suggest was influenced by the inclusion of multiple systems (see Figure 1, panel a). Interestingly, in the multiple-star sample, the rotation break also trends toward 6100 K rather than 6500 K (see Figure 1, panel d), although there is no single preferred rotational boundary in the binary sample:  $-\log_{10}(p)$  remains near its maximum throughout 6100–6500 K. Taken together, these patterns indicate that stellar companions either affect spin-orbit misalignment and alter rotational evolution in a coupled fashion, or bias the inferred  $T_{\text{eff}}$ .

As noted in subsection 2.2, both theoretical models and observational evidence demonstrate that stellar companions *can* efficiently tilt planetary systems. As

suming a representative protoplanetary disk with a disk mass of  $m_{\text{disk}} = 10^{-2} M_{\star}$ , an inner edge at  $a_{\text{in}} = 0.05$  AU and an outer edge at  $a_{\text{out}} = 50$  AU following a surface density profile  $\Sigma \propto r^{-1}$ , together with an eccentricity of  $e' = 0.5$  and a mutual inclination of  $i' = 45^\circ$  between the companion's orbit and the disk, we find<sup>6</sup> that the disk precession timescales are less than, or comparable to, 10 Myr for all misaligned systems (except HAT-P-7, WASP-94, WASP-100, and WASP-180, which have wide-separation and low-mass stellar companions, see Table 1), implying that significant spin-orbit excitation by binary companions is possible (Batygin 2012; Lai 2014). This picture alone, however, does not explain the relatively sharp rise in the misaligned fraction at 6105 K (Figure 1, panel a) unless the companions' properties (e.g., separations, mass ratios, eccentricities) change abruptly near this temperature. Current binary observations lack the temperature resolution needed to test for such a localized step and therefore cannot yet confirm this hypothesis (Offner et al. 2023).

We observe that, although the single-star obliquity transition is determined to be  $T_{\text{eff}} = 6447$  K based on the optimal decision boundary for KS tests, there are two systems cooler than this threshold that are misaligned (Figure 1, panel b): WASP-101 ( $T_{\text{eff}} = 6380 \pm 120$  K,  $\lambda = 34^\circ \pm 3$ ; Zak et al. 2024), and XO-4 ( $T_{\text{eff}} = 6397 \pm 70$  K,  $\lambda = 46.7^{+6.1}_{-8.1}$ ; Narita et al. 2010). Our preceding discussion suggests it to be plausible that these systems host as-yet-unidentified stellar companions. XO-4 has been observed with adaptive optics imaging (Adams et al. 2013) with no companion detected, whereas WASP-101 has not yet been imaged at high angular resolution. Interestingly, the measured  $\lambda$  values for these two systems lie very close to  $35^\circ$ . If we assume  $\lambda \approx \psi$ , these values are consistent with one of two peaks ( $\sim 35^\circ$  and  $\sim 115^\circ$ ) in the obliquity distribution predicted from von Zeipel-Kozai-Lidov cycle simulations (Fabrycky & Tremaine 2007). This coincidence suggests that these systems may indeed host undetected stellar companions; and targeted follow-up observations will be required to confirm or refute this possibility.

Either way, however, it remains puzzling how stellar companions could influence the rotation of the primary star, or tidal interactions with its planets, at the companion orbital separations relevant to our sample. Prior work shows that spin changes are most effective in

close binaries through tidal interactions or companion-induced disk truncation/warping (i.e., at separations  $\lesssim$  a few-tens of AU, Meibom et al. 2007). By contrast, most binaries in our sample have projected separations of order  $10^2$ - $10^3$  AU, in currently standard stellar-evolution recipes, systems at these separations are modeled as effectively isolated stars, with no meaningful cross-influence on interior structure or evolutionary tracks.

Another possibility is that blended photometry/spectroscopy in binaries leads to systematic  $T_{\text{eff}}$  biases (e.g., Andersen 1991; Torres et al. 2010a; El-Badry et al. 2018; Furlan & Howell 2020; Koenigsberger et al. 2025), producing an apparent offset in the obliquity and rotation transitions relative to singles. Interestingly, we found that in our obliquity sample (consisting of hot Jupiters), the planet host is *always* the more massive component of a binary (See Figure 2). This is consistent with the higher hot-Jupiter occurrence around higher-mass stars (Johnson et al. 2010), but it may also reflect detection bias, since transiting planets are more readily found around the brighter primary (e.g., Wang et al. 2019). In such cases, it is tempting to suppose that a close, cooler companion with modest brightness contrast biases the composite spectrum/spectral energy distribution (SED) and drives the inferred  $T_{\text{eff}}$  downward, artificially placing these systems into the “cooler” regime. As shown in the Appendix A, however, the host stars'  $T_{\text{eff}}$  values derived from multi-component SED modeling are consistent with the  $T_{\text{eff}}$  adopted in this work from TEPCat, indicating that contamination of the primary's SED by a stellar companion cannot explain the  $\sim 400$  K  $T_{\text{eff}}$  shift. It is worth noting, however, that the SED fitting relies on spectroscopically derived [Fe/H] priors, which could still be biased by light contamination from stellar companions (El-Badry et al. 2018). Therefore, spatially resolved spectroscopic observations for the binaries listed in Table 1 are required to assess potential spectral contamination affecting the determination of the primaries'  $T_{\text{eff}}$ .

## 5. IMPLICATIONS OF A HIGHER KRAFT BREAK

### 5.1. Few RMs above the single-star Kraft break

A central open question in the study of stellar obliquity, as recently reviewed by Albrecht et al. (2022), is whether spin-orbit misalignments are a byproduct of high-eccentricity migration, and therefore confined to hot-Jupiter-like systems (isolated close-in gas giants plausibly delivered by high-e pathways), or instead reflect a universal process that is largely independent of planetary architecture.

<sup>6</sup> The precession timescales are estimated by interpolating the contour scaling in Figure 3 of Batygin (2012), using representative points along the precession period curves. The code can be found [here](#).

Although, for practical reasons, most RM measurements have targeted hot Jupiters, NASA’s *K2* (Howell et al. 2014) and *TESS* (Ricker et al. 2015) missions have provided suitable targets to extend obliquity measurements beyond hot Jupiters and have revealed intriguing trends.

The emerging picture has so far been that large spin-orbit misalignments concentrate in hot-Jupiter-like, isolated systems (including isolated sub-Saturns that may share high-e delivery channels, Yu & Dai 2024), whereas other categories of planetary systems are typically aligned (see Figure 3), including compact multi-planet systems (Albrecht et al. 2013; Wang et al. 2018; Zhou et al. 2018; Wang et al. 2022; Dai et al. 2023; Lubin et al. 2023; Radzom et al. 2024, 2025), warm Jupiters (Wang et al. 2021; Rice et al. 2022; Wang et al. 2024), eccentric Jupiters (Espinoza-Retamal et al. 2023; Mireles et al. 2025), and very massive close-in companions with  $m_p/M_\star \gtrsim 2 \times 10^{-3}$  (about  $2 M_{\text{Jup}}$  for a solar-mass star, Hébrard et al. 2011; Triaud 2018; Albrecht et al. 2022; Zhou et al. 2019; Rusznak et al. 2025), as well as brown dwarfs (e.g., Giacalone et al. 2024; Ferreira dos Santos et al. 2024; Brady et al. 2025; Carmichael et al. 2025; Doyle et al. 2025; Vowell et al. 2025; Zak et al. 2025). Taken at face value, this contrast may suggest that spin-orbit misalignment is not universally primordial across planetary architectures.

Measuring the spin-orbit (mis)alignments of *non-hot-Jupiter* planets around cool stars, however, provides little discriminating power between these hypotheses, because hot Jupiters around cool stars are also predominantly aligned. A decisive test instead requires obliquity measurements to be taken of non-hot-Jupiter planets around hot hosts. Thus, shifting the single-star Kraft break to  $\sim 6500$  K — and, thereby, changing the boundary between which stars we classify as cool vs. hot — changes the inference we are permitted to draw from the measurements we have in hand. At present there are only five such systems (CoRoT-3,  $T_{\text{eff}}=6558 \pm 44$  K,  $\lambda = -37.6_{-10.0}^{+22.3}$ , Triaud et al. 2009; TOI-3362,  $T_{\text{eff}}=6800 \pm 100$  K,  $\lambda = 1.2_{-2.7}^{+2.8}$ , Espinoza-Retamal et al. 2023; TOI-558,  $T_{\text{eff}}=6466_{-93}^{+95}$  K,  $\lambda = 11.7_{-4.8}^{+7.5}$ , Espinoza-Retamal et al. 2025; TOI-778,  $T_{\text{eff}}=6643 \pm 150$  K,  $\lambda = 18 \pm 11$ , Clark et al. 2023 and WASP-120,  $T_{\text{eff}}=6450 \pm 120$  K,  $\lambda = -2 \pm 4$ , Zak et al. 2024) with RM measurements around stars hotter than our single-star Kraft break, and only one of these (TOI-3362) lies beyond  $1\sigma$  of the break (See Figure 3). With so few robust measurements around genuinely hot stars, the central question — as to whether spin-orbit misalignment is intrinsically more common around hotter stars, regardless of planet type — *remains open*.

A further, albeit tentative, population-level line of evidence that hot stars may be *primordially* more misaligned comes from the distributions of  $v \sin i_\star$  (Louden et al. 2021, 2024) and photometric modulation amplitudes (Mazeh et al. 2015): both are consistent with larger stellar tilts in hotter dwarfs, even for compact multi-planet systems. Moreover, among hot Jupiter hosts, misalignments appear more frequent around A-type than mid-F stars (Albrecht et al. 2022).

One of the strongest remaining arguments against primordial spin-orbit misalignment comes from sub-Saturns around cool stars (see the bottom panel of Figure 3): single sub-Saturns around cool hosts are often misaligned (Winn et al. 2010b; Sanchis-Ojeda & Winn 2011; Bourrier et al. 2022; Stefansson et al. 2022; Knudstrup et al. 2024), whereas compact sub-Saturn multi-planet systems around similar cool hosts are typically well aligned (Radzom et al. 2024, 2025). This contrast indicates that the misalignments of single sub-Saturns around cool stars are most likely dynamical, not primordial. That conclusion, however, should not be naively extrapolated to hot Jupiters, because mechanisms that readily excite the obliquity of a low-mass sub-Saturn do not necessarily operate with comparable efficiency for a massive hot Jupiter.

A concrete example of the perils of such extrapolation is secular resonance crossing (Petrovich et al. 2020), which can drive sub-Saturns onto polar orbits by transferring angular momentum deficit from an outer companion to an inner low-mass planet. Because the inner sub-Saturn carries less orbital angular momentum, its inclination can be strongly excited, whereas a hot Jupiter is much harder to tilt. This mechanism yields a testable prediction: around rapidly rotating hot stars, the stellar quadrupole can dominate over general-relativistic precession, detuning the resonance from exactly polar and driving a characteristic steady-state misalignment near  $65^\circ$ . Observationally, however, no sub-Saturn yet has an RM measurement above  $\sim 6500$  K; recent attempts for TOI-1842 (Wittenmyer et al. 2022; Hixenbaugh et al. 2023) and TOI-1135 (Mallorquín et al. 2024; Dugan et al. 2025) target hosts that are hotter than the previously adopted  $\sim 6100$  K boundary but lie just below the single-star Kraft break at  $\sim 6500$  K, leaving the hot-star prediction (sub-polar clustering near  $\sim 65^\circ$ ) untested.

## 5.2. Obliquity Damping Mechanisms

Our newly attained precision in determining the location of the obliquity transition, complementing that also achieved for the location of the Kraft break, may shed light on the physical origin of the obliquity transi-

tion itself. So far, two tidal mechanisms have been proposed for obliquity damping that predict an obliquity transition — the excitation of inertial waves which are then convectively dissipated (Lai 2012; Saunders et al. 2024), vs. a net orbit-averaged tidal torque exerted by standing internal gravity waves (i.e., g-modes) which are resonance-locked with the orbital frequency (Zanazzi et al. 2024; Zanazzi & Chiang 2025) over the course of the long-term evolution of the Brunt-Väisälä frequency. These proposals are associated with wave propagation and dissipation under different (although largely overlapping) regimes of stellar structure.

In particular, convectively-dissipated obliquity damping predicts an obliquity transition at main-sequence temperatures (and therefore, to leading order, stellar masses) at which stars lose their outer convective envelopes. At this point, magnetic rotational breaking also ceases. Therefore, the obliquity transition should coincide with the rotational Kraft break if this mechanism were solely responsible. By contrast, resonance-locking with g-modes results in an obliquity transition at a stellar mass limit, and therefore main-sequence effective temperature, primarily set by a transition in a specific feature in the long-term evolution of g-mode frequencies. This is most easily described in terms of evolutionary changes to the average Brunt-Väisälä frequency,

$$\langle N \rangle = \int_{\text{rad}} \max(0, N) \frac{dr}{r}, \quad (1)$$

where  $N$  is the Brunt-Väisälä frequency. This integral runs from either the center of the star or the upper boundary of the convective core (if any), to the base of the outer convection zone.

We illustrate this feature of interest in the upper panel of Figure 4, using evolutionary stellar models on either side of this transition. These models<sup>7</sup> were generated with MESA r12778 (Paxton et al. 2011, 2013, 2015, 2018, 2019), using solar-calibrated values of the initial helium abundance and mixing length parameter. Both account for elemental diffusion, and include a small amount of convective overmixing, with  $f_{\text{ov}} = 0.05$ . Over the course of main-sequence evolution, Zanazzi et al. (2024) and Zanazzi & Chiang (2025) show that the averaged Brunt-Väisälä frequencies of cool stars, and therefore all of their g-mode frequencies, increase significantly, gradually, and monotonically over the course of stellar evolution compared to their values  $\langle N_0 \rangle = \langle N(t_0) \rangle$  at some reference epoch  $t_0$  of planet formation. By con-

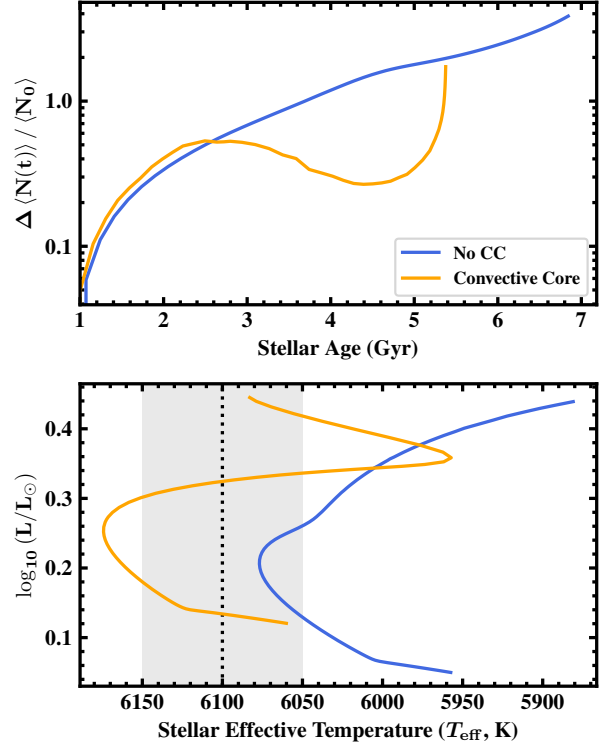


**Figure 4.** Evolution of solar-composition MESA stellar models on either side of the convective-core transition. In both panels, the blue curves show the time evolution of  $1.11 M_{\odot}$  stellar models, which do not exhibit a long-lived convective core on the main sequence, while the orange curves show those of  $1.15 M_{\odot}$  stellar models, where a convective core persists throughout the main sequence until core hydrogen exhaustion. The upper panel shows the time evolution of the average Brunt-Väisälä frequency (or, equivalently, the g-mode undertone spacing), Equation 1, compared to a reference epoch of  $t_0 = 1$  Gyr, as in Zanazzi et al. (2024). The lower panel shows how these stellar models evolve on the Hertzsprung-Russell diagram.

trast, stars that are hotward of the Kraft break have g-modes whose frequencies actually decrease over substantial portions of their main-sequence lifetime, and rapidly increase near main-sequence turnoff. As a result, g-modes in these cool stars are capable of maintaining resonance locks (and, correspondingly, sustaining obliquity-damping torques) during the gradual inward migration of their planets, while those in stars hotward of the Kraft break are not. Thus, were resonance-locking tidal torques to be the dominant mechanism of obliquity damping, an obliquity transition should occur at the same temperature at which this transition in the behaviour of the g-mode frequencies also occurs.

We now make the observation that this transition is distinct from the Kraft break. Both sets of evolutionary models shown in the lower panel of Figure 4

<sup>7</sup> Our MESA inlist files, and a shell script to generate the evolutionary tracks used in this work, have been made available as a deposit on Zenodo.

have very similar stellar masses ( $1.11$  vs  $1.15 M_{\odot}$ ), and very similarly sized convective envelopes, with quite significant depths (reaching to  $0.76$  and  $0.78 R_{\star}$ , respectively). Rather, the cause of this transition is that the lower-mass, cooler, set of evolutionary models is not massive enough to possess a convective core, while the higher-mass set of evolutionary models sustains a convective core throughout its main-sequence lifetime. As in [Zanazzi et al. \(2024\)](#) and [Zanazzi & Chiang \(2025\)](#), our MESA modelling indicates that this transition occurs at a main-sequence effective temperature of roughly  $6100 \pm 100$  K, as can be seen in the lower panel of [Figure 4](#). In general, the location of this stellar-mass boundary is also sensitive to other properties of the star, and to the physics adopted in stellar modelling, in particular the amount of overshooting/convective boundary mixing. However, it is known to be substantially cooler (being at a lower stellar mass) than the rotational Kraft break — e.g. [Silva Aguirre et al. \(2013\)](#); [Bellinger et al. \(2019\)](#); [Buchele et al. \(2025\)](#). So too, therefore, is the obliquity transition predicted by the resonance-locking mechanism alone.

In practice, these two mechanisms are not likely to be mutually exclusive. Both may operate in stars which are cool enough to have convective envelopes and no convective cores ( $T_{\text{eff}} < 6100$  K), and neither in stars with convective cores and no convective envelopes ( $T_{\text{eff}} > 6500$  K). The two misaligned single-star systems discussed in Section 4, with  $6100 < T_{\text{eff}} < 6500$  K, then naturally fall into a regime where only inertial-wave tides operate; the damping is consequently weaker than in cooler stars where both channels are available. Nevertheless, the fact that the Kraft rotation break coincides with the single-star obliquity transition does at least strongly (if circumstantially) suggest that the loss of convective dissipation at higher stellar masses, rather than of resonance locking, is responsible for the obliquity transition.

## 6. CONCLUSION

It is a common working assumption that the stellar-obliquity transition coincides with the rotational Kraft break, motivating the view that obliquity damping in cool stars drives alignment ([Winn et al. 2010a](#); [Albrecht et al. 2012](#); [Winn & Fabrycky 2015](#); [Albrecht et al. 2022](#)). However, it has been noted ([Beyer & White 2024](#)), and our analysis confirms, that the commonly quoted obliquity break near  $T_{\text{eff}} = 6100$  K is several hundred kelvin cooler than the classical rotational break around 6500 K, posing a fundamental inconsistency.

In this work, we have found:

- 1. A unified single-star break at  $\sim 6500$  K.** Restricting to *single stars* (Panel b of [Figure 1](#)), the obliquity transition occurs at  $6447^{+85}_{-119}$  K, in excellent agreement with the single-star rotational Kraft break ( $6510^{+97}_{-127}$  K, panel c of [Figure 1](#)).
- 2. A cooler break arises in multiples.** The  $\sim 6100$  K obliquity break appears when *binaries/multiples* are included (panels a and d of [Figure 1](#)), although the reason is ambiguous (See [section 4](#) for a detailed discussion).

This result is consequential for our understanding of some key issues:

- 1. The origin of spin-orbit misalignment (Hot Jupiter architecture vs. hot hosts).** With the single-star obliquity break revised upward to  $\sim 6500$  K, non-hot-Jupiter RM measurements around *truly* hot hosts ( $T_{\text{eff}} \gtrsim 6500$  K) become extremely sparse (see [Figure 3](#)), leaving open whether large misalignments are unique to Hot Jupiter architectures or broadly common around hot stars.
- 2. The evolution of spin-orbit misalignment (damping mechanism: convective vs. radiative).** The near-perfect coincidence between the single-star obliquity transition and the rotational Kraft break points to a common physical cause: as outer convective envelopes thin toward higher  $T_{\text{eff}}$ , inertial-wave tidal obliquity damping and magnetic braking both weaken, naturally producing simultaneous transitions. The observed coincidence disfavors resonance-locking as the main source of obliquity damping, because it alone would predict an obliquity transition tied to the *convective-core* onset (via g-mode frequency evolution) at  $T_{\text{eff}} = 6100 \pm 100$  K, distinctly cooler than the  $\sim 6500$  K single-star rotation break set by the thinning/vanishing outer convective envelope. We do not, however, claim that these tidal mechanisms must act mutually exclusively; resonance locking may still operate alongside convective-envelope tides in appropriate regimes.

We thank the anonymous reviewer for their constructive feedback, which has greatly improved the quality of this manuscript. We thank Jie Yu and Zheng Guo for bringing the [Beyer & White \(2024\)](#) paper to our attention. We are grateful for helpful discussions with Constantine Deliyannis, Caty Pilachowski, Meng Sun, Cristobal Petrovich, Brandon Radzom, Gongjie Li, Malena Rice, Samir Salim, Zachary Maas, and Timothy Bedding. This work was supported in part by the NASA Exoplanets Research Program NNH23ZDA001N-XRP (Grant No. 80NSSC24K0153), the NASA TESS General Investigator Program, Cycle 7, NNNH23ZDA001N-TESS (Grant No. 80NSSC25K7912), and the Heising-Simons Foundation (Grant #2023-4050). Additionally, X.Y.W. acknowledges support from the Sullivan Prize Fellowship. J.M.J.O. acknowledges support from NASA through the NASA Hubble Fellowship grant HST-HF2-51517.001, awarded by STScI, which is operated by the Association of Universities for Research in Astronomy, Incorporated, under NASA contract NAS5-26555. This research was supported in part by Lilly Endowment, Inc., through its support for the Indiana University Pervasive Technology Institute.

*Facilities:* WIYN/NEID, PFS/Magellan

*Software:* `numpy` ([Oliphant 2006](#); [Walt et al. 2011](#); [Harris et al. 2020](#)), `matplotlib` ([Hunter 2007](#)), `pandas` ([McKinney 2010](#)), `scipy` ([Virtanen et al. 2020](#)), `MESA` ([Paxton et al. 2011, 2013, 2015, 2018, 2019](#))

**Table 1.** Misaligned Hot Jupiters in Binaries or Multi-star systems

Primary	T <sub>eff</sub> adopted by TEPCat				λ	Ref.	Companion	Stellar companions' properties				Primary T <sub>eff</sub> from MS <sup>a</sup>	
	T <sub>eff</sub>	Method <sup>a</sup>	Ref.	(°)				Sep	Sep	Mass	Ref.	ΔMag <sup>f</sup>	T <sub>eff</sub>
(K)				(°)	(")		(AU)	(M <sub>⊕</sub> )				(K)	
<b>Binaries and multiples</b>													
HAT-P-7 A	6310 ± 15	AM	1	155 ± 37	2	B	3.86	1504 <sup>+1377c</sup> <sub>-521</sub>	0.38 <sup>+0.12</sup> <sub>-0.11</sub>	3	8.2 (G)	6360 ± 120	4
HAT-P-14 A	6600 ± 90	SF	5	189.1 ± 5.1	6	B	0.87	180 ± 10	0.20 ± 0.04	7	5.8 (K <sub>s</sub> )	6540 ± 120	4
HAT-P-30 A	6338 ± 42	SF	8	73.5 ± 9.0	9	B	3.83	882 <sup>+430c</sup> <sub>-201</sub>	0.58 <sup>+0.10</sup> <sub>-0.11</sub>	3	4.9 (G)	6190 ± 110	4
HAT-P-32 A	6269 ± 64	MS	10	85 ± 1.5	2	B	2.94	831 ± 15	0.4243 ± 0.0085	7	6.1 (G)	6269 ± 64	10
KELT-4 A	6206 ± 75	MS	11	80 <sup>+25</sup> <sub>-22</sub>	12	B/C <sup>b</sup>	1.5	328 ± 16	0.65 ± 0.10	11	1.4 (K <sub>p</sub> )	6206 ± 75	11
KELT-18 A	6670 ± 120	MS	13	-94.8 ± 0.7	14	B	3.43	1100	0.653 <sup>+0.037d</sup> <sub>-0.04</sub>	13	5.4 (K <sub>p</sub> )	6670 ± 120	13
KELT-23 A	5899 ± 59	MS	15	180.4 <sup>+4.9</sup> <sub>-4.7</sub>	16	B	4.5	570	0.25	15	5.4 (G)	5899 ± 59	15
WASP-12 A	6265 ± 50	SF	17	59 <sup>+15</sup> <sub>-20</sub>	2	B	1.06	462 ± 39	0.554 ± 0.020	7	3.3 (K <sub>s</sub> )	6140 <sup>+130</sup> <sub>-120</sub>	4
						C	1.07	466 ± 40	0.571 ± 0.019	7	3.2 (K <sub>s</sub> )		
WASP-76 A	6329 ± 65	SF	18	-37 <sup>+13</sup> <sub>-21</sub>	18	B	0.44	53.0 ± 8.8	0.712 ± 0.042	19	2.7 (K <sub>s</sub> )	6366 <sup>+92</sup> <sub>-90</sub>	20
WASP-94 A	6170 ± 80	SS	21	151 <sup>+16</sup> <sub>-23</sub>	22	B	16	2700	1.24 ± 0.09	21	0.4 (G)	6170 ± 80	21
WASP-100 A	6940 ± 120	SS	23	79 <sup>+19</sup> <sub>-10</sub>	24	B	3.96	1547 <sup>+895</sup> <sub>-403</sub>	0.45 ± 0.11	3	6.9 (G)	6560 ± 180	4
WASP-136 A	6250 ± 100	SF	25	-38 <sup>+16</sup> <sub>-18</sub>	12	B	5.07	1364	- <sup>e</sup>	26	9.8 (G)	6360 <sup>+150</sup> <sub>-140</sub>	4
WASP-180 A	6500 ± 150	SF	27	-157 ± 2	27	B	5	1200	1	27	0.9 (G)	6150 ± 120	4
<b>Binary candidates</b>													
HAT-P-50	6280 ± 49	SF	28	41 <sup>+10</sup> <sub>-9</sub>	22	B	-	-	-	-	-	-	-
K2-237	6099 ± 110	SF	29	91 ± 7	24	B	-	-	-	-	-	6110 <sup>+120</sup> <sub>-130</sub>	4

\* 1 Benomar et al. (2014), 2 Albrecht et al. (2012), 3 Rice et al. (2024), 4 This work, 5 Torres et al. (2010b), 6 Winn et al. (2011), 7 Ngo et al. (2015), 8 Mortier et al. (2013), 9 Johnson et al. (2011), 10 Zhao et al. (2014), 11 Eastman et al. (2016), 12 Knudstrup et al. (2024), 13 McLeod et al. (2017), 14 Rubenzahl et al. (2024), 15 Johns et al. (2019), 16 Giacalone et al. (2025), 17 Leonardi et al. (2024), 18 Bourrier et al. (2024), 19 Ngo et al. (2016), 20 Fu et al. (2021), 21 Stassun et al. (2017), 22 Neveu-VanMalle et al. (2014), 23 Jansen & Kipping (2020), 24 Addison et al. (2018), 25 Lam et al. (2017), 26 El-Badry et al. (2021), 27 Temple et al. (2019), 28 Hartman et al. (2015), 29 Smith et al. (2019).

<sup>a</sup> AM: asteroseismic modeling, SF: spectra fitting, MS: multi-component SED fitting, SS: single-component SED fitting.

<sup>b</sup> Given that Eastman et al. (2016) estimated KELT-4 B and C to be twin K-type stars, we assume they share identical properties.

<sup>c</sup> This value was derived using `lofti_gaia` (Pearce et al. 2020), incorporating the companion mass reported by Rice et al. (2024) and astrometric measurements (relative RA and DEC, relative proper motions, and *Gaia* parallax) from the *Gaia* DR3 catalog (Gaia Collaboration et al. 2023).

<sup>d</sup> From our multi-component SED modeling.

<sup>e</sup> Only the *Gaia* G magnitude is available, so the stellar mass cannot be derived through isochrone fitting.

<sup>f</sup> G: *Gaia* G band, K<sub>p</sub> or K<sub>s</sub>: Keck NIRC2 K bands.

## APPENDIX

### A. MULTI-COMPONENT SED MODELING FOR SYSTEMS WITH STELLAR COMPANIONS

Based on the misalignment criteria ( $|\lambda| - 2\sigma_\lambda > 0$  and  $|\lambda| > 10^\circ$ ), we identified 15 misaligned hot-Jupiter systems that reside in (candidate) binary or multiple-star systems: HAT-P-7, HAT-P-14, HAT-P-30, HAT-P-32, HAT-P-50, K2-237, KELT-4, KELT-18, KELT-23, WASP-12, WASP-76, WASP-94, WASP-100, WASP-100, and WASP-136. The properties of these systems are listed in Table 1.

The separation between WASP-94 A and WASP-94 B is 15", which is well resolved by *Gaia* DR3 (Gaia Collaboration et al. 2023), 2MASS (Cutri et al. 2003), and WISE (Cutri et al. 2021), and thus light from the stellar companion does not affect the T<sub>eff</sub> determination of the primary. For HAT-P-32 A, KELT-4 A, KELT-18 A, and WASP-76 A, the T<sub>eff</sub> values adopted by TEPCat are derived from multi-component SED fittings. HAT-P-50 is a binary candidate with a *Gaia* DR3 RUWE of 1.4, but no stellar companion has been confirmed, so we cannot estimate the level of possible light contamination from a companion. Therefore, these systems were excluded from our SED analysis.

For HAT-P-7, HAT-P-14, HAT-P-30, WASP-12, WASP-100, and WASP-136, we performed multi-component SED modeling using EXOFASTv2 (Eastman 2017; Eastman et al. 2019) to derived non-contamination SED-based T<sub>eff</sub> for

primary stars. We adopted broadband photometry including *Gaia*  $G$ ,  $G_{\text{bp}}$ ,  $G_{\text{rp}}$ , 2MASS  $JHK$ , and WISE 1–3 for primary stars. For the stellar companions, we included broad photometry from *Gaia* DR3 together with direct imaging measurements (Ngo et al. 2015; McLeod et al. 2017). Gaussian priors on [Fe/H] were derived from the SWEET-Cat catalog (Santos et al. 2013; Sousa et al. 2021), which provides spectroscopic stellar parameters derived from a uniform and homogeneous analysis of the spectra. We assumed that the primary and companion stars share the same initial [Fe/H],  $V$ -band extinction, distance, and age, and adopted the  $V$ -band extinction value from Schlafly & Finkbeiner (2011) as the upper limit on extinction. The *Gaia* DR3 parallax corrected for the zero-point offset, along with its uncertainty (Gaia Collaboration et al. 2023; Lindegren et al. 2021), was adopted as a Gaussian prior on the parallax.

WASP-180 A and B are resolved in *Gaia* DR3, 2MASS, and WISE, but no  $T_{\text{eff}}$  from SED solution is available. We therefore performed single-component SED fit using the aforementioned broad photometry. For KELT-18, although McLeod et al. (2017) performed multi-component SED modeling, they did not report the stellar companion’s mass. We therefore carried out our own multi-component SED modeling to derive it. K2-237 lies in a crowded stellar field, making it impossible to identify bound companions. Therefore, we treated it as a single star and performed single-star SED modeling using *Gaia*  $G$ ,  $G_{\text{bp}}$ ,  $G_{\text{rp}}$ , and 2MASS  $JHK$ , excluding WISE 1–3 photometry due to potential light contamination from nearby stars.

We adopted standard convergence criteria (independent draws  $T_z > 1000$  and Gelman–Rubin statistic  $\hat{R} < 1.01$ ; Eastman et al. 2019). Our analysis, summarized in Table 1, shows that, for primary stars, the  $T_{\text{eff}}$  values from the uncontaminated SED modeling remain consistent, within  $3\sigma$ , with the  $T_{\text{eff}}$  values adopted in this work from TEPCat.

## REFERENCES

Adams, E. R., Dupree, A. K., Kulesa, C., & McCarthy, D. 2013, AJ, 146, 9, doi: [10.1088/0004-6256/146/1/9](https://doi.org/10.1088/0004-6256/146/1/9)

Addison, B. C., Wang, S., Johnson, M. C., et al. 2018, AJ, 156, 197, doi: [10.3847/1538-3881/aade91](https://doi.org/10.3847/1538-3881/aade91)

Albrecht, S., Reffert, S., Quirrenbach, A., Mitchell, D. S., & Snellen, I. 2007, in Astronomical Society of the Pacific Conference Series, Vol. 370, Solar and Stellar Physics Through Eclipses, ed. O. Demircan, S. O. Selam, & B. Albayrak, 218

Albrecht, S., Winn, J. N., Marcy, G. W., et al. 2013, ApJ, 771, 11, doi: [10.1088/0004-637X/771/1/11](https://doi.org/10.1088/0004-637X/771/1/11)

Albrecht, S., Winn, J. N., Johnson, J. A., et al. 2011, ApJ, 738, 50, doi: [10.1088/0004-637X/738/1/50](https://doi.org/10.1088/0004-637X/738/1/50)

—. 2012, ApJ, 757, 18, doi: [10.1088/0004-637X/757/1/18](https://doi.org/10.1088/0004-637X/757/1/18)

Albrecht, S. H., Dawson, R. I., & Winn, J. N. 2022, PASP, 134, 082001, doi: [10.1088/1538-3873/ac6c09](https://doi.org/10.1088/1538-3873/ac6c09)

Albrecht, S. H., Marcussen, M. L., Winn, J. N., Dawson, R. I., & Knudstrup, E. 2021, ApJL, 916, L1, doi: [10.3847/2041-8213/ac0f03](https://doi.org/10.3847/2041-8213/ac0f03)

Andersen, J. 1991, A&A Rv, 3, 91, doi: [10.1007/BF00873538](https://doi.org/10.1007/BF00873538)

Anderson, D. R., Bouchy, F., Brown, D. J. A., et al. 2018, arXiv e-prints, arXiv:1812.09264, doi: [10.48550/arXiv.1812.09264](https://doi.org/10.48550/arXiv.1812.09264)

Avallone, E. A., Tayar, J. N., van Saders, J. L., et al. 2022, ApJ, 930, 7, doi: [10.3847/1538-4357/ac60a1](https://doi.org/10.3847/1538-4357/ac60a1)

Barnes, S. A. 2003, ApJ, 586, 464, doi: [10.1086/367639](https://doi.org/10.1086/367639)

Batygin, K. 2012, Nature, 491, 418, doi: [10.1038/nature11560](https://doi.org/10.1038/nature11560)

Bellinger, E. P., Basu, S., Hekker, S., & Christensen-Dalsgaard, J. 2019, ApJ, 885, 143, doi: [10.3847/1538-4357/ab4a0d](https://doi.org/10.3847/1538-4357/ab4a0d)

Benomar, O., Masuda, K., Shibahashi, H., & Suto, Y. 2014, PASJ, 66, 94, doi: [10.1093/pasj/psu069](https://doi.org/10.1093/pasj/psu069)

Beyer, A. C., & White, R. J. 2024, ApJ, 973, 28, doi: [10.3847/1538-4357/ad6b0d](https://doi.org/10.3847/1538-4357/ad6b0d)

Boesgaard, A. M., & Tripicco, M. J. 1986, ApJL, 302, L49, doi: [10.1086/184635](https://doi.org/10.1086/184635)

Bouchy, F., Moutou, C., Queloz, D., & CoRoT Exoplanet Science Team. 2009, in IAU Symposium, Vol. 253, Transiting Planets, ed. F. Pont, D. Sasselov, & M. J. Holman, 129–139, doi: [10.1017/S174392130802632X](https://doi.org/10.1017/S174392130802632X)

Bourrier, V., Lovis, C., Cretignier, M., et al. 2021, A&A, 654, A152, doi: [10.1051/0004-6361/202141527](https://doi.org/10.1051/0004-6361/202141527)

Bourrier, V., Zapatero Osorio, M. R., Allart, R., et al. 2022, A&A, 663, A160, doi: [10.1051/0004-6361/202142559](https://doi.org/10.1051/0004-6361/202142559)

Bourrier, V., Delisle, J.-B., Lovis, C., et al. 2024, A&A, 691, A113, doi: [10.1051/0004-6361/202449203](https://doi.org/10.1051/0004-6361/202449203)

Brady, M., Bean, J. L., Stefánsson, G., et al. 2025, AJ, 169, 64, doi: [10.3847/1538-3881/adc66](https://doi.org/10.3847/1538-3881/adc66)

Brown, D. J. A., Collier Cameron, A., Díaz, R. F., et al. 2012, ApJ, 760, 139, doi: [10.1088/0004-637X/760/2/139](https://doi.org/10.1088/0004-637X/760/2/139)

Brun, A. S., & Browning, M. K. 2017, Living Reviews in Solar Physics, 14, 4, doi: [10.1007/s41116-017-0007-8](https://doi.org/10.1007/s41116-017-0007-8)

Buchele, L., Bellinger, E. P., Hekker, S., & Basu, S. 2025, ApJ, 987, 97, doi: [10.3847/1538-4357/add697](https://doi.org/10.3847/1538-4357/add697)

Carmichael, T. W., Giacalone, S., Vowell, N., et al. 2025, arXiv e-prints, arXiv:2506.18971, doi: [10.48550/arXiv.2506.18971](https://doi.org/10.48550/arXiv.2506.18971)

Cegla, H. M., Lovis, C., Bourrier, V., et al. 2016, *A&A*, 588, A127, doi: [10.1051/0004-6361/201527794](https://doi.org/10.1051/0004-6361/201527794)

Chaplin, W. J., & Miglio, A. 2013, *ARA&A*, 51, 353, doi: [10.1146/annurev-astro-082812-140938](https://doi.org/10.1146/annurev-astro-082812-140938)

Christiansen, J. L., McElroy, D. L., Harbut, M., et al. 2025, arXiv e-prints, arXiv:2506.03299, doi: [10.48550/arXiv.2506.03299](https://doi.org/10.48550/arXiv.2506.03299)

Clark, J. T., Addison, B. C., Okumura, J., et al. 2023, *AJ*, 165, 207, doi: [10.3847/1538-3881/acc3a0](https://doi.org/10.3847/1538-3881/acc3a0)

Collier Cameron, A., Bruce, V. A., Miller, G. R. M., Triaud, A. H. M. J., & Queloz, D. 2010, *MNRAS*, 403, 151, doi: [10.1111/j.1365-2966.2009.16131.x](https://doi.org/10.1111/j.1365-2966.2009.16131.x)

Cox, J. P. 1980, *Theory of Stellar Pulsation*. (PSA-2), Volume 2, Vol. 2

Cutri, R. M., Skrutskie, M. F., van Dyk, S., et al. 2003, *VizieR Online Data Catalog*, II/246

Cutri, R. M., Wright, E. L., Conrow, T., et al. 2021, *VizieR Online Data Catalog: AllWISE Data Release (Cutri+ 2013)*, *VizieR On-line Data Catalog: II/328*. Originally published in: IPAC/Caltech (2013)

Dai, F., Masuda, K., Beard, C., et al. 2023, *AJ*, 165, 33, doi: [10.3847/1538-3881/aca327](https://doi.org/10.3847/1538-3881/aca327)

Dalal, S., Hébrard, G., Lecavelier des Étangs, A., et al. 2019, *A&A*, 631, A28, doi: [10.1051/0004-6361/201935944](https://doi.org/10.1051/0004-6361/201935944)

Deliyannis, C. P., & Pinsonneault, M. H. 1997, *ApJ*, 488, 836, doi: [10.1086/304747](https://doi.org/10.1086/304747)

do Nascimento, Jr., J. D., Charbonnel, C., Lèbre, A., de Laverny, P., & De Medeiros, J. R. 2000, *A&A*, 357, 931, doi: [10.48550/arXiv.astro-ph/0003010](https://doi.org/10.48550/arXiv.astro-ph/0003010)

Doyle, L., Cañas, C. I., Libby-Roberts, J. E., et al. 2025, *MNRAS*, 536, 3745, doi: [10.1093/mnras/stae2819](https://doi.org/10.1093/mnras/stae2819)

Dugan, E., Wang, X.-Y., Heron, A., et al. 2025, arXiv e-prints, arXiv:2510.20740, doi: [10.48550/arXiv.2510.20740](https://doi.org/10.48550/arXiv.2510.20740)

Eastman, J. 2017, EXOFASTv2: Generalized publication-quality exoplanet modeling code. <http://ascl.net/1710.003>

Eastman, J. D., Beatty, T. G., Siverd, R. J., et al. 2016, *AJ*, 151, 45, doi: [10.3847/0004-6256/151/2/45](https://doi.org/10.3847/0004-6256/151/2/45)

Eastman, J. D., Rodriguez, J. E., Agol, E., et al. 2019, arXiv e-prints, arXiv:1907.09480. <https://arxiv.org/abs/1907.09480>

El-Badry, K., Rix, H.-W., & Heintz, T. M. 2021, *MNRAS*, 506, 2269, doi: [10.1093/mnras/stab323](https://doi.org/10.1093/mnras/stab323)

El-Badry, K., Rix, H.-W., Ting, Y.-S., et al. 2018, *MNRAS*, 473, 5043, doi: [10.1093/mnras/stx2758](https://doi.org/10.1093/mnras/stx2758)

Espinoza-Retamal, J. I., Brahm, R., Petrovich, C., et al. 2023, *ApJL*, 958, L20, doi: [10.3847/2041-8213/ad096d](https://doi.org/10.3847/2041-8213/ad096d)

Espinoza-Retamal, J. I., Jordán, A., Brahm, R., et al. 2025, *AJ*, 170, 70, doi: [10.3847/1538-3881/ade22e](https://doi.org/10.3847/1538-3881/ade22e)

Fabrycky, D., & Tremaine, S. 2007, *ApJ*, 669, 1298, doi: [10.1086/521702](https://doi.org/10.1086/521702)

Feinstein, A. D., Montet, B. T., Ansdel, M., et al. 2020, *AJ*, 160, 219, doi: [10.3847/1538-3881/abac0a](https://doi.org/10.3847/1538-3881/abac0a)

Ferreira dos Santos, T., Rice, M., Wang, X.-Y., & Wang, S. 2024, *AJ*, 168, 145, doi: [10.3847/1538-3881/ad6b7f](https://doi.org/10.3847/1538-3881/ad6b7f)

Fontanive, C., & Bardalez Gagliuffi, D. 2021, *Frontiers in Astronomy and Space Sciences*, 8, 16, doi: [10.3389/fspas.2021.625250](https://doi.org/10.3389/fspas.2021.625250)

Frémat, Y., Royer, F., Marchal, O., et al. 2023, *A&A*, 674, A8, doi: [10.1051/0004-6361/202243809](https://doi.org/10.1051/0004-6361/202243809)

Fu, G., Deming, D., Lothringer, J., et al. 2021, *AJ*, 162, 108, doi: [10.3847/1538-3881/ac1200](https://doi.org/10.3847/1538-3881/ac1200)

Fulton, B. J., Howard, A. W., Winn, J. N., et al. 2013, *ApJ*, 772, 80, doi: [10.1088/0004-637X/772/2/80](https://doi.org/10.1088/0004-637X/772/2/80)

Furlan, E., & Howell, S. B. 2020, *ApJ*, 898, 47, doi: [10.3847/1538-4357/ab9c9c](https://doi.org/10.3847/1538-4357/ab9c9c)

Gaia Collaboration, Vallenari, A., Brown, A. G. A., et al. 2023, *A&A*, 674, A1, doi: [10.1051/0004-6361/202243940](https://doi.org/10.1051/0004-6361/202243940)

Giacalone, S., Dai, F., Zanazzi, J. J., et al. 2024, *AJ*, 168, 189, doi: [10.3847/1538-3881/ad785a](https://doi.org/10.3847/1538-3881/ad785a)

Giacalone, S., Howard, A. W., Rubenzahl, R. A., et al. 2025, *PASP*, 137, 074401, doi: [10.1088/1538-3873/adecc2](https://doi.org/10.1088/1538-3873/adecc2)

Guenther, E. W., Díaz, R. F., Gazzano, J. C., et al. 2012, *A&A*, 537, A136, doi: [10.1051/0004-6361/201117706](https://doi.org/10.1051/0004-6361/201117706)

Gupta, A. F., Millholland, S. C., Im, H., et al. 2024, *Nature*, 632, 50, doi: [10.1038/s41586-024-07688-3](https://doi.org/10.1038/s41586-024-07688-3)

Harris, C. R., Millman, K. J., van der Walt, S. J., et al. 2020, *Nature*, 585, 357

Hartman, J. D., Bhatti, W., Bakos, G. Á., et al. 2015, *AJ*, 150, 168, doi: [10.1088/0004-6256/150/6/168](https://doi.org/10.1088/0004-6256/150/6/168)

Hébrard, G., Ehrenreich, D., Bouchy, F., et al. 2011, *A&A*, 527, L11, doi: [10.1051/0004-6361/201016331](https://doi.org/10.1051/0004-6361/201016331)

Hixenbaugh, K., Wang, X.-Y., Rice, M., & Wang, S. 2023, *ApJL*, 949, L35, doi: [10.3847/2041-8213/acd6f5](https://doi.org/10.3847/2041-8213/acd6f5)

Hobbs, L. M., & Pilachowski, C. 1986, *ApJL*, 309, L17, doi: [10.1086/184752](https://doi.org/10.1086/184752)

Hodges, J. L. 1958, *Arkiv för Matematik*, 3, 469. <https://api.semanticscholar.org/CorpusID:121451525>

Holman, M., Touma, J., & Tremaine, S. 1997, *Nature*, 386, 254, doi: [10.1038/386254a0](https://doi.org/10.1038/386254a0)

Howell, S. B., Sobeck, C., Haas, M., et al. 2014, *PASP*, 126, 398, doi: [10.1086/676406](https://doi.org/10.1086/676406)

Hunter, J. D. 2007, *Computing in science & engineering*, 9, 90

Iben, Jr., I. 1967, *ApJ*, 147, 650, doi: [10.1086/149041](https://doi.org/10.1086/149041)

Jansen, T., & Kipping, D. 2020, *MNRAS*, 494, 4077, doi: [10.1093/mnras/staa814](https://doi.org/10.1093/mnras/staa814)

Johns, D., Reed, P. A., Rodriguez, J. E., et al. 2019, *AJ*, 158, 78, doi: [10.3847/1538-3881/ab24c7](https://doi.org/10.3847/1538-3881/ab24c7)

Johnson, J. A., Aller, K. M., Howard, A. W., & Crepp, J. R. 2010, PASP, 122, 905, doi: [10.1086/655775](https://doi.org/10.1086/655775)

Johnson, J. A., Winn, J. N., Bakos, G. Á., et al. 2011, ApJ, 735, 24, doi: [10.1088/0004-637X/735/1/24](https://doi.org/10.1088/0004-637X/735/1/24)

Johnson, M. C., Cochran, W. D., Addison, B. C., Tinney, C. G., & Wright, D. J. 2017, AJ, 154, 137, doi: [10.3847/1538-3881/aa8462](https://doi.org/10.3847/1538-3881/aa8462)

Kawaler, S. D. 1989, ApJL, 343, L65, doi: [10.1086/185512](https://doi.org/10.1086/185512)

Kjeldsen, H., & Bedding, T. R. 1995, A&A, 293, 87, doi: [10.48550/arXiv.astro-ph/9403015](https://doi.org/10.48550/arXiv.astro-ph/9403015)

Knudstrup, E., Albrecht, S. H., Winn, J. N., et al. 2024, A&A, 690, A379, doi: [10.1051/0004-6361/202450627](https://doi.org/10.1051/0004-6361/202450627)

Koenigsberger, G., Schmutz, W., Pilachowski, C., et al. 2025, arXiv e-prints, arXiv:2507.19954, doi: [10.48550/arXiv.2507.19954](https://doi.org/10.48550/arXiv.2507.19954)

Kraft, R. P. 1967, ApJ, 150, 551, doi: [10.1086/149359](https://doi.org/10.1086/149359)

Lai, D. 2012, MNRAS, 423, 486, doi: [10.1111/j.1365-2966.2012.20893.x](https://doi.org/10.1111/j.1365-2966.2012.20893.x)

—. 2014, MNRAS, 440, 3532, doi: [10.1093/mnras/stu485](https://doi.org/10.1093/mnras/stu485)

Lam, K. W. F., Faedi, F., Brown, D. J. A., et al. 2017, A&A, 599, A3, doi: [10.1051/0004-6361/201629403](https://doi.org/10.1051/0004-6361/201629403)

Leonardi, P., Nascimbeni, V., Granata, V., et al. 2024, A&A, 686, A84, doi: [10.1051/0004-6361/202348363](https://doi.org/10.1051/0004-6361/202348363)

Li, G., & Winn, J. N. 2016, ApJ, 818, 5, doi: [10.3847/0004-637X/818/1/5](https://doi.org/10.3847/0004-637X/818/1/5)

Lindegren, L., Hernández, J., Bombrun, A., et al. 2018, A&A, 616, A2, doi: [10.1051/0004-6361/201832727](https://doi.org/10.1051/0004-6361/201832727)

Lindegren, L., Klioner, S. A., Hernández, J., et al. 2021, A&A, 649, A2, doi: [10.1051/0004-6361/202039709](https://doi.org/10.1051/0004-6361/202039709)

Louden, E. M., Winn, J. N., Petigura, E. A., et al. 2021, AJ, 161, 68, doi: [10.3847/1538-3881/abcebd](https://doi.org/10.3847/1538-3881/abcebd)

Louden, E. M., Wang, S., Winn, J. N., et al. 2024, ApJL, 968, L2, doi: [10.3847/2041-8213/ad4b1b](https://doi.org/10.3847/2041-8213/ad4b1b)

Lubin, J., Wang, X.-Y., Rice, M., et al. 2023, ApJL, 959, L5, doi: [10.3847/2041-8213/ad0fea](https://doi.org/10.3847/2041-8213/ad0fea)

Mallorquí, M., Lodieu, N., Béjar, V. J. S., et al. 2024, A&A, 685, A90, doi: [10.1051/0004-6361/202349016](https://doi.org/10.1051/0004-6361/202349016)

Mamajek, E. E., & Hillenbrand, L. A. 2008, ApJ, 687, 1264, doi: [10.1086/591785](https://doi.org/10.1086/591785)

Mancini, L., Esposito, M., Covino, E., et al. 2022, A&A, 664, A162, doi: [10.1051/0004-6361/202243742](https://doi.org/10.1051/0004-6361/202243742)

Mathur, S., Santos, Á. R. G., Claytor, Z. R., et al. 2025, ApJ, 982, 114, doi: [10.3847/1538-4357/adb8cc](https://doi.org/10.3847/1538-4357/adb8cc)

Mazeh, T., Perets, H. B., McQuillan, A., & Goldstein, E. S. 2015, ApJ, 801, 3, doi: [10.1088/0004-637X/801/1/3](https://doi.org/10.1088/0004-637X/801/1/3)

McKinney, W. 2010, in Proceedings of the 9th Python in Science Conference, Vol. 445, Austin, TX, 51–56

McLaughlin, D. B. 1924, ApJ, 60, 22, doi: [10.1086/142826](https://doi.org/10.1086/142826)

McLeod, K. K., Rodriguez, J. E., Oelkers, R. J., et al. 2017, AJ, 153, 263, doi: [10.3847/1538-3881/aa6d5d](https://doi.org/10.3847/1538-3881/aa6d5d)

Meibom, S., Mathieu, R. D., & Stassun, K. G. 2007, ApJL, 665, L155, doi: [10.1086/521437](https://doi.org/10.1086/521437)

Mireles, I., Murgas, F., Dragomir, D., et al. 2025, arXiv e-prints, arXiv:2509.22972, doi: [10.48550/arXiv.2509.22972](https://doi.org/10.48550/arXiv.2509.22972)

Mortier, A., Santos, N. C., Sousa, S. G., et al. 2013, A&A, 558, A106, doi: [10.1051/0004-6361/201322240](https://doi.org/10.1051/0004-6361/201322240)

Naoz, S., Farr, W. M., & Rasio, F. A. 2012, The Astrophysical Journal Letters, 754, L36

Narita, N., Hirano, T., Sanchis-Ojeda, R., et al. 2010, PASJ, 62, L61, doi: [10.1093/pasj/62.6.L61](https://doi.org/10.1093/pasj/62.6.L61)

NASA Exoplanet Archive. 2019, Composite Planet Data Table, IPAC, doi: [10.26133/NEA2](https://doi.org/10.26133/NEA2)

Neveu-VanMalle, M., Queloz, D., Anderson, D. R., et al. 2014, A&A, 572, A49, doi: [10.1051/0004-6361/201424744](https://doi.org/10.1051/0004-6361/201424744)

Newton, E. R., Irwin, J., Charbonneau, D., et al. 2017, ApJ, 834, 85, doi: [10.3847/1538-4357/834/1/85](https://doi.org/10.3847/1538-4357/834/1/85)

Ngo, H., Knutson, H. A., Hinkley, S., et al. 2015, ApJ, 800, 138, doi: [10.1088/0004-637X/800/2/138](https://doi.org/10.1088/0004-637X/800/2/138)

—. 2016, ApJ, 827, 8, doi: [10.3847/0004-637X/827/1/8](https://doi.org/10.3847/0004-637X/827/1/8)

Nordström, B., Mayor, M., Andersen, J., et al. 2004, A&A, 418, 989, doi: [10.1051/0004-6361:20035959](https://doi.org/10.1051/0004-6361:20035959)

Noyes, R. W., Hartmann, L. W., Baliunas, S. L., Duncan, D. K., & Vaughan, A. H. 1984, ApJ, 279, 763, doi: [10.1086/161945](https://doi.org/10.1086/161945)

Offner, S. S. R., Moe, M., Kratter, K. M., et al. 2023, in Astronomical Society of the Pacific Conference Series, Vol. 534, Protostars and Planets VII, ed. S. Inutsuka, Y. Aikawa, T. Muto, K. Tomida, & M. Tamura, 275, doi: [10.48550/arXiv.2203.10066](https://doi.org/10.48550/arXiv.2203.10066)

Ogilvie, G. I., & Lin, D. N. C. 2007, ApJ, 661, 1180, doi: [10.1086/515435](https://doi.org/10.1086/515435)

Oliphant, T. E. 2006, A guide to NumPy, Vol. 1 (Trelgol Publishing USA)

Paxton, B., Bildsten, L., Dotter, A., et al. 2011, ApJS, 192, 3, doi: [10.1088/0067-0049/192/1/3](https://doi.org/10.1088/0067-0049/192/1/3)

Paxton, B., Cantiello, M., Arras, P., et al. 2013, ApJS, 208, 4, doi: [10.1088/0067-0049/208/1/4](https://doi.org/10.1088/0067-0049/208/1/4)

Paxton, B., Marchant, P., Schwab, J., et al. 2015, ApJS, 220, 15, doi: [10.1088/0067-0049/220/1/15](https://doi.org/10.1088/0067-0049/220/1/15)

Paxton, B., Schwab, J., Bauer, E. B., et al. 2018, ApJS, 234, 34, doi: [10.3847/1538-4365/aaa5a8](https://doi.org/10.3847/1538-4365/aaa5a8)

Paxton, B., Smolec, R., Schwab, J., et al. 2019, ApJS, 243, 10, doi: [10.3847/1538-4365/ab2241](https://doi.org/10.3847/1538-4365/ab2241)

Pearce, L. A., Kraus, A. L., Dupuy, T. J., et al. 2020, ApJ, 894, 115, doi: [10.3847/1538-4357/ab8389](https://doi.org/10.3847/1538-4357/ab8389)

Petrovich, C., Muñoz, D. J., Kratter, K. M., & Malhotra, R. 2020, ApJL, 902, L5, doi: [10.3847/2041-8213/abb952](https://doi.org/10.3847/2041-8213/abb952)

Pizzolato, N., Maggio, A., Micela, G., Sciortino, S., & Ventura, P. 2003, *A&A*, 397, 147, doi: [10.1051/0004-6361:20021560](https://doi.org/10.1051/0004-6361:20021560)

Pont, F., Endl, M., Cochran, W. D., et al. 2010, *MNRAS*, 402, L1, doi: [10.1111/j.1745-3933.2009.00785.x](https://doi.org/10.1111/j.1745-3933.2009.00785.x)

Radzom, B. T., Dong, J., Rice, M., et al. 2025, *AJ*, 169, 189, doi: [10.3847/1538-3881/ad9dd5](https://doi.org/10.3847/1538-3881/ad9dd5)

—. 2024, *AJ*, 168, 116, doi: [10.3847/1538-3881/ad61d8](https://doi.org/10.3847/1538-3881/ad61d8)

Reiners, A., Basri, G., & Browning, M. 2009, *ApJ*, 692, 538, doi: [10.1088/0004-637X/692/1/538](https://doi.org/10.1088/0004-637X/692/1/538)

Rice, M., Gerbig, K., & Vanderburg, A. 2024, arXiv e-prints, arXiv:2401.04173, doi: [10.48550/arXiv.2401.04173](https://doi.org/10.48550/arXiv.2401.04173)

Rice, M., Wang, S., Wang, X.-Y., et al. 2022, *AJ*, 164, 104, doi: [10.3847/1538-3881/ac8153](https://doi.org/10.3847/1538-3881/ac8153)

Ricker, G. R., Winn, J. N., Vanderspek, R., et al. 2015, *Journal of Astronomical Telescopes, Instruments, and Systems*, 1, 014003, doi: [10.1117/1.JATIS.1.1.014003](https://doi.org/10.1117/1.JATIS.1.1.014003)

Rossiter, R. A. 1924, *ApJ*, 60, 15, doi: [10.1086/142825](https://doi.org/10.1086/142825)

Rubenzahl, R. A., Dai, F., Halverson, S., et al. 2024, *AJ*, 168, 188, doi: [10.3847/1538-3881/ad70b5](https://doi.org/10.3847/1538-3881/ad70b5)

Rusznak, J., Wang, X.-Y., Rice, M., & Wang, S. 2025, *ApJL*, 983, L42, doi: [10.3847/2041-8213/adc129](https://doi.org/10.3847/2041-8213/adc129)

Saar, S. H., & Brandenburg, A. 1999, *ApJ*, 524, 295, doi: [10.1086/307794](https://doi.org/10.1086/307794)

Sanchis-Ojeda, R., & Winn, J. N. 2011, *ApJ*, 743, 61, doi: [10.1088/0004-637X/743/1/61](https://doi.org/10.1088/0004-637X/743/1/61)

Santos, N. C., Sousa, S. G., Mortier, A., et al. 2013, *A&A*, 556, A150, doi: [10.1051/0004-6361/201321286](https://doi.org/10.1051/0004-6361/201321286)

Saunders, N., Grunblatt, S. K., Chontos, A., et al. 2024, *AJ*, 168, 81, doi: [10.3847/1538-3881/ad543b](https://doi.org/10.3847/1538-3881/ad543b)

Schlafly, E. F., & Finkbeiner, D. P. 2011, *ApJ*, 737, 103, doi: [10.1088/0004-637X/737/2/103](https://doi.org/10.1088/0004-637X/737/2/103)

Schlaufman, K. C. 2010, *ApJ*, 719, 602, doi: [10.1088/0004-637X/719/1/602](https://doi.org/10.1088/0004-637X/719/1/602)

Schröder, C., Reiners, A., & Schmitt, J. H. M. M. 2009, *A&A*, 493, 1099, doi: [10.1051/0004-6361:200810377](https://doi.org/10.1051/0004-6361:200810377)

Schwarz, R., Funk, B., Zechner, R., & Bazsó, Á. 2016, *MNRAS*, 460, 3598, doi: [10.1093/mnras/stw1218](https://doi.org/10.1093/mnras/stw1218)

See, V., Roquette, J., Amard, L., & Matt, S. 2023, *MNRAS*, 524, 5781, doi: [10.1093/mnras/stad2020](https://doi.org/10.1093/mnras/stad2020)

Sestito, P., & Randich, S. 2005, *A&A*, 442, 615, doi: [10.1051/0004-6361:20053482](https://doi.org/10.1051/0004-6361:20053482)

Siegel, J. C., Winn, J. N., & Albrecht, S. H. 2023, *ApJL*, 950, L2, doi: [10.3847/2041-8213/acd62f](https://doi.org/10.3847/2041-8213/acd62f)

Silva Aguirre, V., Basu, S., Brandão, I. M., et al. 2013, *ApJ*, 769, 141, doi: [10.1088/0004-637X/769/2/141](https://doi.org/10.1088/0004-637X/769/2/141)

Simpson, E. K., Pollacco, D., Cameron, A. C., et al. 2011, *MNRAS*, 414, 3023, doi: [10.1111/j.1365-2966.2011.18603.x](https://doi.org/10.1111/j.1365-2966.2011.18603.x)

Skumanich, A. 1972, *ApJ*, 171, 565, doi: [10.1086/151310](https://doi.org/10.1086/151310)

Smith, A. M. S., Csizmadia, S., Gandolfi, D., et al. 2019, *AcA*, 69, 135, doi: [10.32023/0001-5237/69.2.3](https://doi.org/10.32023/0001-5237/69.2.3)

Sousa, S. G., Adibekyan, V., Delgado-Mena, E., et al. 2021, *A&A*, 656, A53, doi: [10.1051/0004-6361/202141584](https://doi.org/10.1051/0004-6361/202141584)

Southworth, J. 2011, *MNRAS*, 417, 2166, doi: [10.1111/j.1365-2966.2011.19399.x](https://doi.org/10.1111/j.1365-2966.2011.19399.x)

Spalding, C., & Winn, J. N. 2022, *ApJ*, 927, 22, doi: [10.3847/1538-4357/ac4993](https://doi.org/10.3847/1538-4357/ac4993)

Stassun, K. G., Collins, K. A., & Gaudi, B. S. 2017, *AJ*, 153, 136, doi: [10.3847/1538-3881/aa5df3](https://doi.org/10.3847/1538-3881/aa5df3)

Stefansson, G., Mahadevan, S., Petrovich, C., et al. 2022, *ApJL*, 931, L15, doi: [10.3847/2041-8213/ac6e3c](https://doi.org/10.3847/2041-8213/ac6e3c)

Stelzer, B., Damasso, M., Scholz, A., & Matt, S. P. 2016, *MNRAS*, 463, 1844, doi: [10.1093/mnras/stw1936](https://doi.org/10.1093/mnras/stw1936)

Struve, O., & Elvey, C. T. 1931, *MNRAS*, 91, 663, doi: [10.1093/mnras/91.6.663](https://doi.org/10.1093/mnras/91.6.663)

Taylor, J., Claytor, Z. R., Huber, D., & van Saders, J. 2022, *ApJ*, 927, 31, doi: [10.3847/1538-4357/ac4bbc](https://doi.org/10.3847/1538-4357/ac4bbc)

Temple, L. Y., Hellier, C., Anderson, D. R., et al. 2019, *MNRAS*, 490, 2467, doi: [10.1093/mnras/stz2632](https://doi.org/10.1093/mnras/stz2632)

Teng, H.-Y., Dai, F., Howard, A. W., et al. 2025, *AJ*, 170, 51, doi: [10.3847/1538-3881/addrab9](https://doi.org/10.3847/1538-3881/addrab9)

Torres, G., Andersen, J., & Giménez, A. 2010a, *A&A Rv*, 18, 67, doi: [10.1007/s00159-009-0025-1](https://doi.org/10.1007/s00159-009-0025-1)

Torres, G., Bakos, G. Á., Hartman, J., et al. 2010b, *ApJ*, 715, 458, doi: [10.1088/0004-637X/715/1/458](https://doi.org/10.1088/0004-637X/715/1/458)

Triaud, A. H. M. J. 2018, in *Handbook of Exoplanets*, ed. H. J. Deeg & J. A. Belmonte, 2, doi: [10.1007/978-3-319-55333-7\\_2](https://doi.org/10.1007/978-3-319-55333-7_2)

Triaud, A. H. M. J., Queloz, D., Bouchy, F., et al. 2009, *A&A*, 506, 377, doi: [10.1051/0004-6361/200911897](https://doi.org/10.1051/0004-6361/200911897)

Triaud, A. H. M. J., Collier Cameron, A., Queloz, D., et al. 2010, *A&A*, 524, A25, doi: [10.1051/0004-6361/201014525](https://doi.org/10.1051/0004-6361/201014525)

Triaud, A. H. M. J., Queloz, D., Hellier, C., et al. 2011, *A&A*, 531, A24, doi: [10.1051/0004-6361/201016367](https://doi.org/10.1051/0004-6361/201016367)

van Saders, J. L., & Pinsonneault, M. H. 2013, *ApJ*, 776, 67, doi: [10.1088/0004-637X/776/2/67](https://doi.org/10.1088/0004-637X/776/2/67)

van Saders, J. L., Pinsonneault, M. H., & Barbieri, M. 2019, *ApJ*, 872, 128, doi: [10.3847/1538-4357/aaafae](https://doi.org/10.3847/1538-4357/aaafae)

Vidotto, A. A., Gregory, S. G., Jardine, M., et al. 2014, *MNRAS*, 441, 2361, doi: [10.1093/mnras/stu728](https://doi.org/10.1093/mnras/stu728)

Virtanen, P., Gommers, R., Oliphant, T. E., et al. 2020, *Nature methods*, 17, 261

Vowell, N., Dong, J., Rodriguez, J. E., et al. 2025, arXiv e-prints, arXiv:2510.00105, doi: [10.48550/arXiv.2510.00105](https://doi.org/10.48550/arXiv.2510.00105)

Walt, S. v. d., Colbert, S. C., & Varoquaux, G. 2011, *Computing in Science & Engineering*, 13, 22

Wang, S., Addison, B., Fischer, D. A., et al. 2018, AJ, 155, 70, doi: [10.3847/1538-3881/aaa2fb](https://doi.org/10.3847/1538-3881/aaa2fb)

Wang, S., Jones, M., Shporer, A., et al. 2019, AJ, 157, 51, doi: [10.3847/1538-3881/aaf1b7](https://doi.org/10.3847/1538-3881/aaf1b7)

Wang, S., Winn, J. N., Addison, B. C., et al. 2021, AJ, 162, 50, doi: [10.3847/1538-3881/ac0626](https://doi.org/10.3847/1538-3881/ac0626)

Wang, X.-Y., Rice, M., Wang, S., et al. 2022, ApJL, 926, L8, doi: [10.3847/2041-8213/ac4f44](https://doi.org/10.3847/2041-8213/ac4f44)

—. 2024, ApJL, 973, L21, doi: [10.3847/2041-8213/ad7469](https://doi.org/10.3847/2041-8213/ad7469)

Weber, E. J., & Davis, Jr., L. 1967, ApJ, 148, 217, doi: [10.1086/149138](https://doi.org/10.1086/149138)

Westgate, C. 1934, ApJ, 79, 357, doi: [10.1086/143542](https://doi.org/10.1086/143542)

Winn, J. N., Fabrycky, D., Albrecht, S., & Johnson, J. A. 2010a, ApJL, 718, L145, doi: [10.1088/2041-8205/718/2/L145](https://doi.org/10.1088/2041-8205/718/2/L145)

Winn, J. N., & Fabrycky, D. C. 2015, ARA&A, 53, 409, doi: [10.1146/annurev-astro-082214-122246](https://doi.org/10.1146/annurev-astro-082214-122246)

Winn, J. N., Howard, A. W., Johnson, J. A., et al. 2009, ApJ, 703, 2091, doi: [10.1088/0004-637X/703/2/2091](https://doi.org/10.1088/0004-637X/703/2/2091)

Winn, J. N., Johnson, J. A., Howard, A. W., et al. 2010b, ApJL, 723, L223, doi: [10.1088/2041-8205/723/2/L223](https://doi.org/10.1088/2041-8205/723/2/L223)

Winn, J. N., Howard, A. W., Johnson, J. A., et al. 2011, AJ, 141, 63, doi: [10.1088/0004-6256/141/2/63](https://doi.org/10.1088/0004-6256/141/2/63)

Wittenmyer, R. A., Clark, J. T., Trifonov, T., et al. 2022, AJ, 163, 82, doi: [10.3847/1538-3881/ac3f39](https://doi.org/10.3847/1538-3881/ac3f39)

Wu, Y., & Murray, N. 2003, ApJ, 589, 605, doi: [10.1086/374598](https://doi.org/10.1086/374598)

Wyttenbach, A., Lovis, C., Ehrenreich, D., et al. 2017, A&A, 602, A36, doi: [10.1051/0004-6361/201630063](https://doi.org/10.1051/0004-6361/201630063)

Yu, H., & Dai, F. 2024, ApJ, 972, 159, doi: [10.3847/1538-4357/ad5ffb](https://doi.org/10.3847/1538-4357/ad5ffb)

Zak, J., Boffin, H. M. J., Bocchieri, A., et al. 2025, arXiv e-prints, arXiv:2505.20516, doi: [10.48550/arXiv.2505.20516](https://doi.org/10.48550/arXiv.2505.20516)

Zak, J., Bocchieri, A., Sedaghati, E., et al. 2024, A&A, 686, A147, doi: [10.1051/0004-6361/202349084](https://doi.org/10.1051/0004-6361/202349084)

Zanazzi, J. J., & Chiang, E. 2025, ApJ, 983, 157, doi: [10.3847/1538-4357/adc114](https://doi.org/10.3847/1538-4357/adc114)

Zanazzi, J. J., Dewberry, J., & Chiang, E. 2024, ApJL, 967, L29, doi: [10.3847/2041-8213/ad4644](https://doi.org/10.3847/2041-8213/ad4644)

Zhao, M., O'Rourke, J. G., Wright, J. T., et al. 2014, ApJ, 796, 115, doi: [10.1088/0004-637X/796/2/115](https://doi.org/10.1088/0004-637X/796/2/115)

Zhou, G., Bayliss, D., Hartman, J. D., et al. 2015, ApJL, 814, L16, doi: [10.1088/2041-8205/814/1/L16](https://doi.org/10.1088/2041-8205/814/1/L16)

Zhou, G., Rodriguez, J. E., Collins, K. A., et al. 2016, AJ, 152, 136, doi: [10.3847/0004-6256/152/5/136](https://doi.org/10.3847/0004-6256/152/5/136)

Zhou, G., Rodriguez, J. E., Vanderburg, A., et al. 2018, AJ, 156, 93, doi: [10.3847/1538-3881/aad085](https://doi.org/10.3847/1538-3881/aad085)

Zhou, G., Bakos, G. Á., Bayliss, D., et al. 2019, AJ, 157, 31, doi: [10.3847/1538-3881/aaf1bb](https://doi.org/10.3847/1538-3881/aaf1bb)